A Coupled Finite Element Analysis of Independently Modeled Substructures by Penalty Frame Method

Maenghyo Cho*
School of Mechanical and Aerospace Engineering, Seoul National University, Seoul 151-742, Korea
Won Bae Kim
Department of Aerospace Engineering, Inha University, 253 Yong-Hyun Dong Nam-Ku, Inchon 402-751, Korea

A penalty frame method is proposed for the coupled analysis of finite elements with independently modeled substructures. Although previously reported hybrid interface method by Aminpour et al (IJNME, Vol 38, 1995) is accurate and reliable, it requires non-conventional special solution algorithm such as multifrontal solver. In present study, an alternative method has been developed using penalty frame constraints, which results in positive symmetric global stiffness matrices. Thus the conventional skyline solver or band solver can be utilized in the solution routine, which makes the present method applicable in the environment of conventional finite element commercial software. Numerical examples show applicability of the present method.

Key Words: Penalty Frame Method, Substructure, Domain Coupled Analysis, Finite Element

1. Introduction

In a detailed structural design stage, reliable and efficient stress analysis are required. To reduce computational effort and modeling complexity, global-local methods are frequently employed in the current structural computations. They are multi-point constraint method (Kris-hnamurthy and Raju, 1992), mesh overlay method (Fish, 1992; Robbins and Reddy, 1992), Lagrange multiplier method (Farhat and Roux, 1991), and transition element method (Surana, 1980).

Conventional global-local analysis is limited to the problems with the mesh conformity in the interface between global and local zones. However, there are some cases in which coupled analyses are required. The assembled structural systems requires a coupled analysis in which the effect of interactions between substructures should be considered. Usually, in the aircraft industry, each substructure is analyzed by different groups independently. Thus the meshes of each substructure may not coincide at the interfaces between adjacent substructures.

Recently, a reliable coupled analysis method has been proposed to analyze structures with independently modeled finite element subdomains by Aminpour et al (1995). This method does not require one-to-one nodal correspondence on the subdomain boundaries. Thus it provides modeling flexibility and eliminates the need for complex mesh transitioning.

The present study is motivated by this hybrid interface technology (Aminpour et al., 1995; Aminpour et al., 1992; Ransom and McCleary, 1993; Aminpour and Krishnamurthy, 1997; Ransom, 1997; Wang and Ransom, 1997) currently

* Corresponding Author,
E-mail: mhcho@snu.ac.kr
TEL: +82-2-880-1693; **FAX**: +82-2-883-1513
School of Mechanical and Aerospace Engineering, Seoul National University, Seoul 151-742, Korea. (Manuscript **Received** March 8, 2001; **Revised** July 2, 2002)

available. The hybrid interface method provides reliable computational tool which already demonstrated its applicability to the material and geometric nonlinear problems in the previously reported articles (Aminpour and Krishnamurthy, 1997 ; Ransom, 1997 ; Wang and Ransom, 1997) in 2-D and 3-D applications. It appears that this method can be extended to more complicated problems with nonlinearity of materials and deformations. However, the hybrid interface method has its own drawbacks. As the other hybrid finite element formulations, the formulation of hybrid interface method is quite complicated. This method does not generate banded global stiffness matrices and the global stiffness matrices are not positive definite. Thus for the efficient solution method, special algorithms such as multi-frontal solver are required because the $\mathbf{LDL}^T$ Choleski decomposition cannot be applied.

Thus the objective of present study is to develop interface methodology which can provide efficient coupled finite element analyses. We propose a "penally frame method". In the interfaces between independently modeled finite element meshes, displacement continuity conditions are imposed by penalty function constraints.

Interface frame elements are introduced to apply connectivity conditions of displacements of one substructure to the other. The present formulation provides a symmetric banded positive definite global stiffness matrices for the global coupled system. Thus conventional direct solution algorithm known as skyline solver is applicable for coupled analysis. By applying the present method, a great amount of saving of computing time and memory are expected in the mesh-coupled large scale problems.

The drawbacks of the previously developed hybrid interface method are now circumvented by the present penalty method. The present penalty frame method can work as an efficient and reliable interface matching tool for the coupled analysis of independently modeled substructures.

2. Formulation

The interface between two mesh configurations

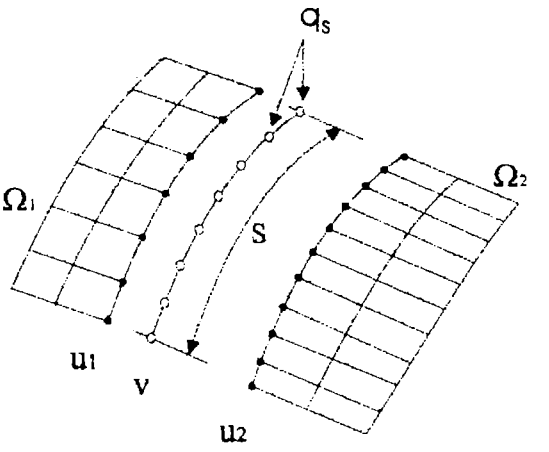

Fig. 1 Interface element configuration

is given in Fig. 1. To satisfy the traction continuity conditions at the interface between substructures, in the weak form, the hybrid interface method introduces a Lagrange multiplier λ. On the other hand, present penalty method does not require satisfaction of interface traction conditions. The displacement continuity constraints are imposed only through penalty parameters. Thus formulation of the present penalty frame method is simpler than that of hybrid method because it does not employ additional interface unknowns λ and it preserves symmetric banded nature of global stiffness matrix which cannot be expected at the presence of Lagrange multiplier in the formulation.

The variational statement for the present method is given in the following form.

$$\Pi = \Pi_{\Omega_1} + \Pi_{\Omega_2} + \frac{1}{2}\int_s (\mathbf{v}-\mathbf{u})^T k (\mathbf{v}-\mathbf{u})\, ds \quad (1)$$

The frame displacement $\mathbf{v}$ and subdomain displacement field $\mathbf{u}$ can be approximated as

$$\mathbf{v} = \mathbf{T}\mathbf{q}_s, \qquad \mathbf{u} = \mathbf{N}_j \mathbf{q}_j \quad (2)$$

where $\mathbf{T}$ and $\mathbf{N}_j$ are shape functions of $\mathbf{v}$ and $\mathbf{u}$.

The individual substructure potential energy can be expressed as follows.

$$\Pi_{\Omega_i} = \frac{1}{2}\mathbf{q}_i^T \mathbf{K}_i \mathbf{q}_i - \mathbf{q}_i^T \mathbf{f}_i = \frac{1}{2}\begin{bmatrix}\mathbf{q}_i^T & \mathbf{q}_i^{oT}\end{bmatrix}\begin{bmatrix}\mathbf{K}_i^a & \mathbf{K}_i^b \\ \mathbf{K}_i^{bT} & \mathbf{K}_i^{\infty}\end{bmatrix}\begin{bmatrix}\mathbf{q}_i \\ \mathbf{q}_i^o\end{bmatrix} - \begin{bmatrix}\mathbf{q}_i^T & \mathbf{q}_i^{oT}\end{bmatrix}\begin{bmatrix}\mathbf{f}_i \\ \mathbf{f}_i^o\end{bmatrix} \quad (3)$$

$$\Pi_{\Omega_2}=\frac{1}{2}\mathbf{q}_2^T\mathbf{K}_2\mathbf{q}_2-\mathbf{q}_2^T\mathbf{f}_2$$
$$=\frac{1}{2}\begin{bmatrix}\mathbf{q}_2^{iT} & \mathbf{q}_2^{oT}\end{bmatrix}\begin{bmatrix}\mathbf{K}_2^{ii} & \mathbf{K}_2^{io}\\ \mathbf{K}_2^{oi} & \mathbf{K}_2^{oo}\end{bmatrix}\begin{bmatrix}\mathbf{q}_2^{i}\\ \mathbf{q}_2^{o}\end{bmatrix}-\begin{bmatrix}\mathbf{q}_2^{iT} & \mathbf{q}_2^{oT}\end{bmatrix}\begin{bmatrix}\mathbf{f}_2^{i}\\ \mathbf{f}_2^{o}\end{bmatrix} \quad (4)$$

The stationary condition is obtained by taking the first variation with respect to the independent degrees of freedom ($\mathbf{q}_j^o$, $\mathbf{q}_j^i$ and $\mathbf{q}_s$).

$$\delta\Pi\,|_{\mathbf{q}^o_1,\mathbf{q}^i_1,\mathbf{q}_s,\mathbf{q}^o_2,\mathbf{q}^i_2}=\delta\Pi_{\Omega_1}+\delta\Pi_{\Omega_2}+k\int_S\{\delta\mathbf{v}^T-\delta\mathbf{u}^T\}(\mathbf{v}-\mathbf{u})\,ds$$
$$=\begin{bmatrix}\delta\mathbf{q}_1^{iT} & \delta\mathbf{q}_1^{oT}\end{bmatrix}\left\{\begin{bmatrix}\mathbf{K}_1^{ii} & \mathbf{K}_1^{io}\\ \mathbf{K}_1^{oi} & \mathbf{K}_1^{oo}\end{bmatrix}\begin{bmatrix}\mathbf{q}_1^{i}\\ \mathbf{q}_1^{o}\end{bmatrix}-\begin{bmatrix}\mathbf{f}_1^{i}\\ \mathbf{f}_1^{o}\end{bmatrix}\right\}$$
$$+\begin{bmatrix}\delta\mathbf{q}_2^{iT} & \delta\mathbf{q}_2^{oT}\end{bmatrix}\left\{\begin{bmatrix}\mathbf{K}_2^{ii} & \mathbf{K}_2^{io}\\ \mathbf{K}_2^{oi} & \mathbf{K}_2^{oo}\end{bmatrix}\begin{bmatrix}\mathbf{q}_2^{i}\\ \mathbf{q}_2^{o}\end{bmatrix}-\begin{bmatrix}\mathbf{f}_2^{i}\\ \mathbf{f}_2^{o}\end{bmatrix}\right\} \quad (5)$$
$$+\begin{bmatrix}\delta\mathbf{q}_s^{T} & \delta\mathbf{q}_j^{iT}\end{bmatrix}\begin{bmatrix}\mathbf{G}_j^{ss} & \mathbf{G}_j^{isT}\\ \mathbf{G}_j^{is} & \mathbf{G}_j^{ii}\end{bmatrix}\begin{bmatrix}\mathbf{q}_s\\ \mathbf{q}_j^{i}\end{bmatrix}=0$$

where

$$\mathbf{G}_j^{is}=k_j\int_S\mathbf{N}_j^T\mathbf{T}_j ds,$$
$$\mathbf{G}_j^{ii}=k_j\int_S\mathbf{N}_j^T\mathbf{N}_j ds \text{ and } \mathbf{G}_j^{ss}=k_j\int_S\mathbf{T}_j^T\mathbf{T}_j ds \quad (6)$$

$\mathbf{q}_j^o$ and $\mathbf{q}_j^i$ are the generalized displacement in subdomain Ω_j. Superscript o indicates the subdomain quantities which are not on the interfaces and superscript i denotes the subdomain degrees of freedom which is on the interfaces. $\mathbf{q}_s$ is the generalized displacement along the penalty frame and $\mathbf{K}_1$ and $\mathbf{K}_2$ are stiffness matrices of each subdomain. Global stiffness equation can be rearranged and be expressed as,

$$\begin{bmatrix}\mathbf{K}_1^{oo} & \mathbf{K}_1^{oi} & 0 & 0 & 0\\ \mathbf{K}_1^{io} & \mathbf{K}_1^{ii}+\mathbf{G}_1^{ii} & -\mathbf{G}_1^{is} & 0 & 0\\ 0 & -\mathbf{G}_1^{si} & \mathbf{G}_1^{ss}+\mathbf{G}_2^{ss} & -\mathbf{G}_2^{si} & 0\\ 0 & 0 & -\mathbf{G}_2^{is} & \mathbf{K}_2^{ii}+\mathbf{G}_2^{ii} & \mathbf{K}_2^{io}\\ 0 & 0 & 0 & \mathbf{K}_2^{oi} & \mathbf{K}_2^{oo}\end{bmatrix}\begin{Bmatrix}\mathbf{q}_1^o\\ \mathbf{q}_1^i\\ \mathbf{q}_s\\ \mathbf{q}_2^i\\ \mathbf{q}_2^o\end{Bmatrix}=\begin{Bmatrix}\mathbf{f}_1^o\\ \mathbf{f}_1^i\\ 0\\ \mathbf{f}_2^i\\ \mathbf{f}_2^o\end{Bmatrix} \quad (7)$$

The displacement field $\mathbf{v}$ on the frame interface is interpolated using new shape function $\mathbf{T}$ and nodal displacement $\mathbf{q}_s$. Piecewise linear functions and cubic spline functions are employed as interpolation functions of $\mathbf{T}$. In the case of using cubic spline function, it is necessary to compute the values of the first and second derivatives of the interface displacement $\mathbf{v}$ at the ends of the interface. In the present study these derivatives are computed by applying finite difference of the interface nodal values at the end.

$$\mathbf{v}=f(s)=\sum_{i=-1}^{n}c_iB_i(s)=\sum_{i=-1}^{n}B_i(s)\,[A]f_i \quad (8)$$

In the above Eq. (8), $n+2$ spline function B_i and coefficient of spline function c_i are required in the condition of the given n data set. To determine the $n+2$ coefficients c_i, the $n+2$ equations are required. But we have only n data set. Thus to get additional two more conditions it is required to extract the values of first or second derivatives at both ends of interface. The $n+2$ conditions are expressed as $[A]f_i$ in Eq. (8), in which the dimension of the matrix $[A]$ is $(n+2)\times n$. The coefficient f_i is the interface nodal displacement value which is the component of $\mathbf{q}_s$.

The cubic spline function B_i is defined as follows.

if $t\in[t_{i-2},\ t_{i-1}]$,
$$B_i(t)=\frac{1}{h^3}\{(t-t_{i-2})^3\}$$

if $t\in[t_{i-1},\ t_i]$,
$$B_i(t)=\frac{1}{h^3}\{h^3+3h^2(t-t_{i-1})+3h(t-t_{i-1})^2-3(t-t_{i-1})^3\}$$

if $t\in[t_i,\ t_{i+1}]$,
$$B_i(t)=\frac{1}{h^3}\{h^3+3h^2(t_{i+1}-t)+3h(t_{i+1}-t)^2-3(t_{i+1}-t)^3\}$$

if $t\in[t_{i+1},\ t_{i+2}]$,
$$B_i(t)=\frac{1}{h^3}\{(t_{i+2}-t)^3\}$$

otherwise, $B_i=0$ (9)

where h denotes the length of the interval between the nodes on the frame interface.

On the other hand, the variational statement for the hybrid interface method is given in the following form. The detailed derivations can be found in the reference (Aminpour et al., 1995).

$$\Pi=\Pi_{\Omega_1}+\Pi_{\Omega_2}+\int_S\boldsymbol{\lambda}^T(\mathbf{v}-\mathbf{u})\,ds \quad (10)$$

$$\boldsymbol{\lambda}=\mathbf{R}\boldsymbol{\alpha} \quad (11)$$

where $\mathbf{R}$ is the base function of $\boldsymbol{\lambda}$ and $\boldsymbol{\alpha}$ is the parameter vector to be determined. The stationary condition is obtained for the independent degrees of freedom ($\mathbf{q}_j^o$, $\mathbf{q}_j^i$, $\mathbf{q}_s$, and $\boldsymbol{\alpha}$).

$$\delta\Pi\,|_{\mathbf{q}^o_1,\mathbf{q}^i_1,\mathbf{q}_s,\mathbf{q}^o_2,\mathbf{q}^i_2,\boldsymbol{\alpha}}=0 \quad (12)$$

$$\begin{bmatrix} \mathbf{K}_1^{ii} & \mathbf{K}_1^{io} & 0 & 0 & 0 & \mathbf{M}_1 & 0 \\ \mathbf{K}_1^{oi} & \mathbf{K}_1^{oo} & 0 & 0 & 0 & 0 & 0 \\ 0 & 0 & \mathbf{K}_2^{ii} & \mathbf{K}_2^{io} & 0 & 0 & \mathbf{M}_2 \\ 0 & 0 & \mathbf{K}_2^{oi} & \mathbf{K}_2^{oo} & 0 & 0 & 0 \\ 0 & 0 & 0 & 0 & 0 & \mathbf{G}_1 & \mathbf{G}_2 \\ \mathbf{M}_1^T & 0 & 0 & 0 & \mathbf{G}_1^T & 0 & 0 \\ 0 & 0 & \mathbf{M}_2^T & 0 & \mathbf{G}_2^T & 0 & 0 \end{bmatrix} \begin{Bmatrix} \mathbf{q}_1^i \\ \mathbf{q}_1^o \\ \mathbf{q}_2^i \\ \mathbf{q}_2^o \\ \mathbf{q}_s \\ \alpha_1 \\ \alpha_2 \end{Bmatrix} = \begin{Bmatrix} \mathbf{f}_1^i \\ \mathbf{f}_1^o \\ \mathbf{f}_2^i \\ \mathbf{f}_2^o \\ 0 \\ 0 \\ 0 \end{Bmatrix} \quad (13)$$

where

$$\mathbf{M}_j = -\int_S \mathbf{N}_j^T \mathbf{R}_j ds \text{ and } \mathbf{G}_j = -\int_S \mathbf{T}_j^T \mathbf{R}_j ds \; ; \; j = 1, 2 \quad (14)$$

Some of the diagonal component of the global stiffness matrix is zero in the hybrid interface method as given in Eq. (13).

However, no zero diagonal component can be found in the present formulation which is given in Eq. (7). While the hybrid interface method produces non-banded and positive indefinite global stiffness matrices as shown in Eq. (13), the present penalty frame method produces symmetric banded positive definite stiffness matrices as shown in Eq. (7). Thus this method does not require complicated special solver such as multi-frontal solver. The present penalty method facilitates direct solver such as Gauss-elimination after $\mathbf{LDL}^T$ decomposition of the global stiffness matrices.

3. Numerical Examples

Various numerical examples are tested to assess the efficiency and accuracy of the present method. Linear piecewise polynomials and cubic splines are used as the interpolation functions in the interface frame elements for the numerical computations for the newly proposed method. However, various types of interpolation functions can also be easily applied for the base functions of the interface displacement field **v**.

3.1 Cantilever beam with a vertical interface

This numerical example is the one of simplest problem to check validity of the proposed method. The configuration of geometry and mesh is depicted in the Fig. 2. Four-node isoparametric elements are used. Only end stretching and shear loads are considered.

Table 1 Numerical result for beam extension

Mesh a	Mesh b	disp.(u_{tip})	Penalty Frame
10×8	10×3	6.00	pass the patch test
10×8	10×4	6.00	pass the patch test
10×8	10×5	6.00	pass the patch test
Exact		6.00	

Table 2 Numerical result for beam flexure

	Mesh a	Mesh b	disp.(v_{tip})
Conventional	10×2	10×2	98.46
Finite	10×4	10×4	99.91
Element	10×8	10×8	100.32
Penalty	10×4	10×2	99.42
Frame	10×8	10×2	99.89
Method	10×8	10×4	100.22
Exact	-		102.60

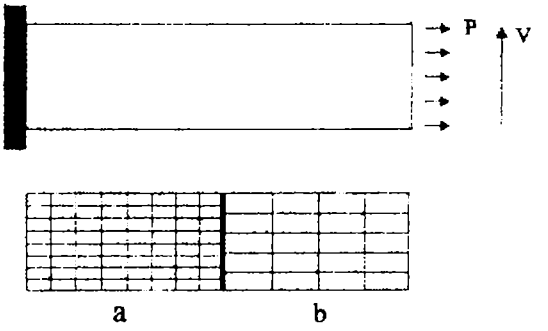

Fig. 2 Cantilever beam with a vertical interface under extension or shear load

In the interface frame, three nodes are placed with the equal spaces. Since the number of frame nodes has no importance in this case, all the simulation results with the number of interface nodes greater than three are the same as the exact patch solutions. As shown in Table 1, present analysis with node mismatching at the interface of subdomains pass the patch test for uniform extension case. Thus the present method share the patch-passing capability with the hybrid interface method.

The flexure test also shows the validity of the present penalty approach. Table 2 describes mesh configuration for the coupled analysis. For the various mesh configurations, it is observed that the end deflections were obtained accurately. The

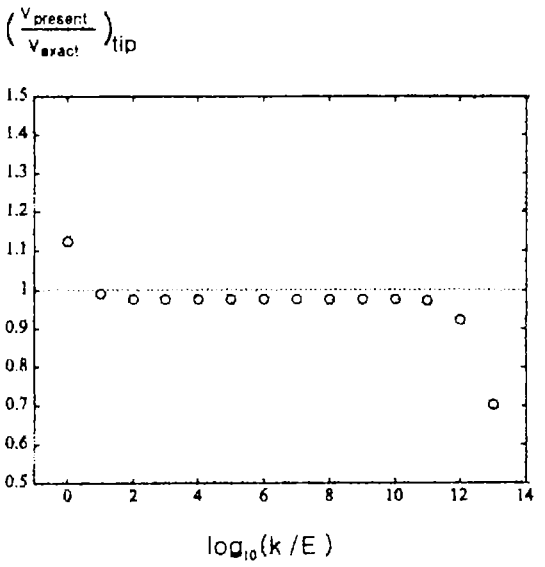

Fig. 3 Sensitivity of penalty parameter for beam bending problem with tip load

displacement results of the coupled analysis are almost equivalent to those of the uniform mesh configuration. The displacement results of the present approach show close agreement with those of the exact elasticity solution.

The stable range of penalty parameter k is examined in Fig. 3. As shown in Fig. 3, stable end deflection v is provided in the wide range of penalty parameter, $10^2 < k/E < 10^{10}$. This implies the newly developed method works insensitively for the wide range of the values of the penalty parameter.

3.2 Plate with a center hole

Plate with a central circular hole under uniform tension load is considered. It is a well-established stress concentration problem to investigate the performance of coupled analysis. The configuration of the whole geometry and local zone is shown in the Fig. 4. The coupled global-local analysis demonstrates the accuracy and reliability of the proposed method.

It provides accurate prediction for stress concentration factors as shown in Fig. 5. In Fig. 5, $(N_x)_o$ denotes uniform far-field longitudinal stress resultant. N_θ is the distributions of the hoop stress resultant along the $\theta=0$ line (along the x axis).

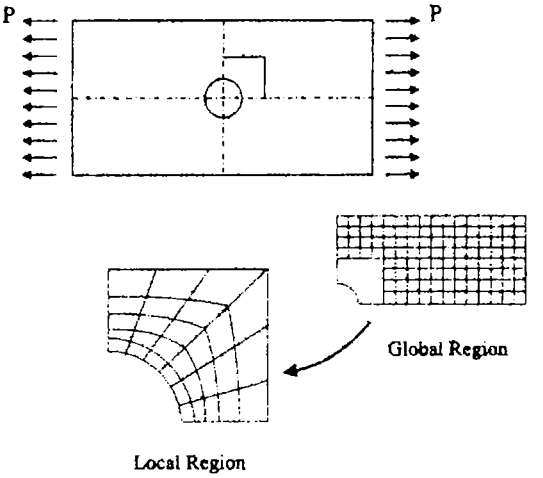

Fig. 4 Plate with a center hole

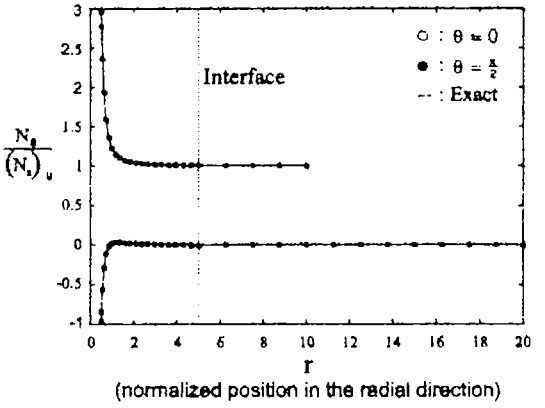

Fig. 5 Stress concentration factor along radius

The coordinate r represents the normalized position in the radial direction with respect to the hole radius R_o. Hoop stress distribution of the plate with circular hole $(H/R_o=4.0)$ is given in the plotting. In the local zone, the number of nodes in the radial direction is 21 and the number of nodes in the circumferential direction is 21. In the interface frame between global and local zone, 13 nodes are placed in equal spaces. The stress concentration factor $K_f(=N_\theta/(N_x)_o)$ of the present method shows good correlation with that of the elasticity solution.

As shown in Fig. 6, the range of validity of penalty parameter has been investigated. Stable solutions were obtained for dimensionless parameter $10^2 < k/E < 10^{10}$. Once more, the variation

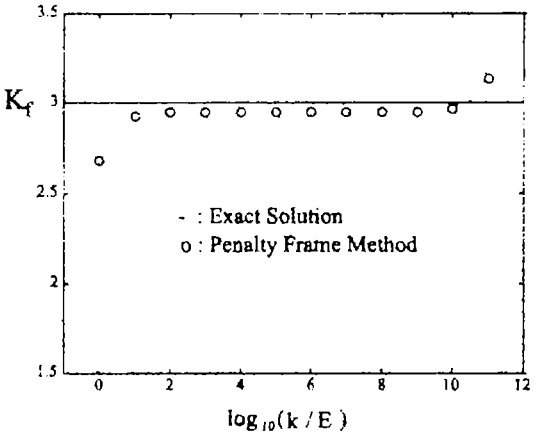

Fig. 6 Sensitivity of dimensionless penalty parameters for plate problem with a hole

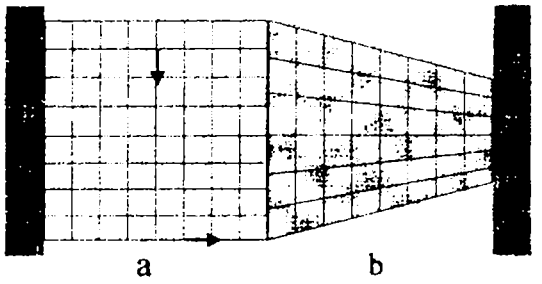

Fig. 7 Clamped-clamped unsymmetric beam

of the penalty parameter does not make sensitive influence on the accuracy of the solutions.

3.3 Clamped-clamped unsymmetric beam

Here, we consider clamped-clamped unsymmetric beam problem as shown in Fig. 7. This problem was tested using Hybrid variational method for parallel computing in reference (Farhat and Geradin, 1992). It has two substructures, which have different material constants and mesh configurations, and two ends are clamped.

Substructure **a** has 16 by 16 mesh, and the mesh of substructure **b** is 12 by 16. For the case of the ratio of Young's modulus in substructure **a** and **b** is 0.2 ($E_a/E_b=0.2$), the displacement results are shown in the Fig. 8 to the Fig. 15. Substructure **a** has 17 interface nodes, substructure **b** has 13, and the number of interface frame nodes are 17.

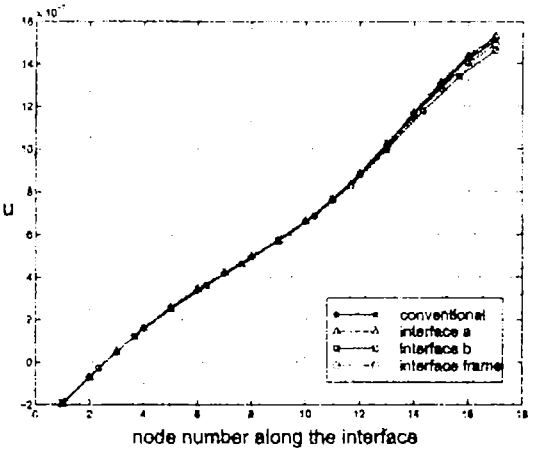

Fig. 8 Horizontal displacement u along the interface ($k/E=10^1$)

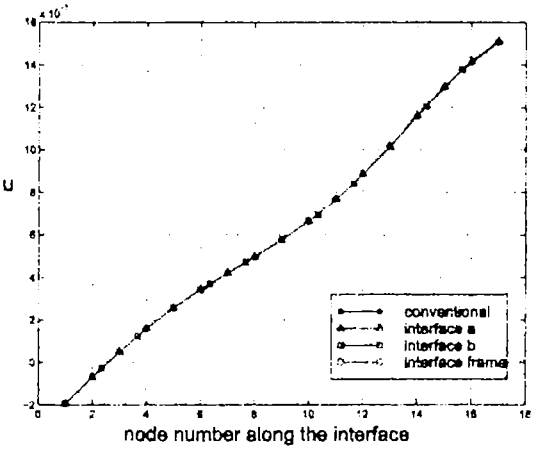

Fig. 9 Horizontal displacement u along the interface ($k/E=10^2$)

For the four different values of penalty parameters, the numerical computations were carried out. Figures 9 and 13 show the optimal performance for the interface displacement solutions with the penalty parameter $k/E=10^2$. For the smaller penalty parameter ($k/E=10^1$), penalty constraints are not strong enough to provide reliable solutions as shown in Figs. 8 and 12.

Special attention needs to be paid on the cases of larger penalty parameter ($k/E=10^4$) than the optimal value ($k/E=10^2$). In those cases ($k/E>10^4$), although the horizontal displacement of coupled substructure analysis agree reasonably well with those of compatible finite element

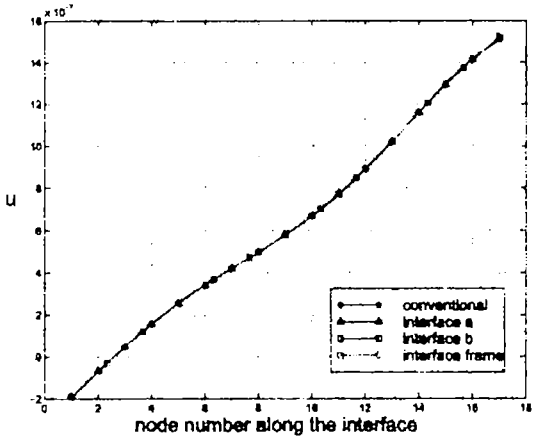

Fig. 10 Horizontal displacement u along the interface $(k/E=10^3)$

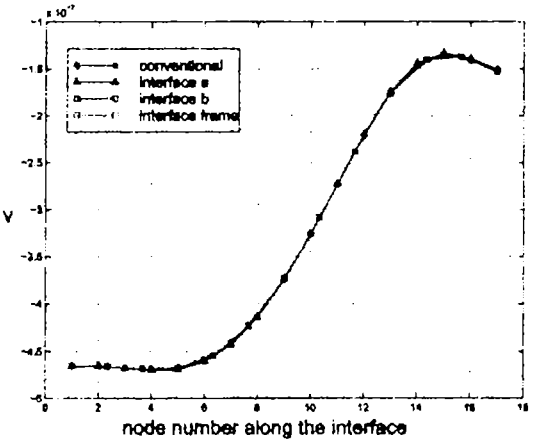

Fig. 13 Vertical displacement v along the interface $(k/E=10^2)$

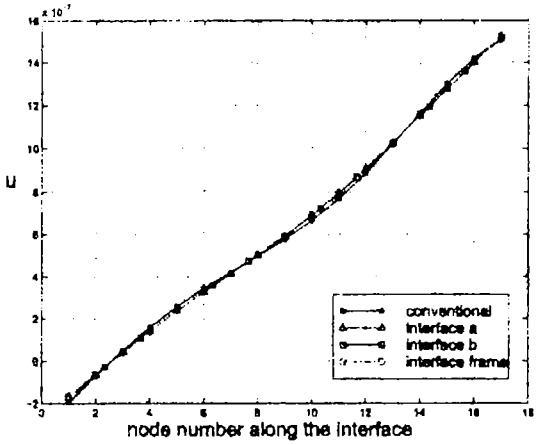

Fig. 11 Horizontal displacement u along the interface $(k/E=10^4)$

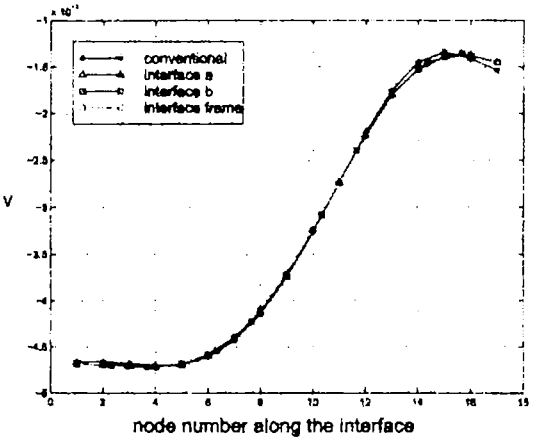

Fig. 14 Vertical displacement v along the interface $(k/E=10^3)$

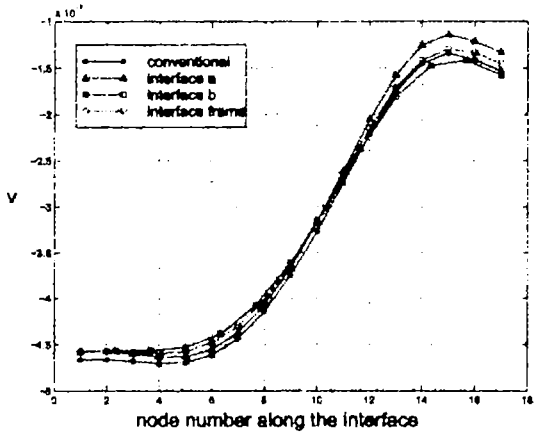

Fig. 12 Vertical displacement v along the interface $(k/E=10^1)$

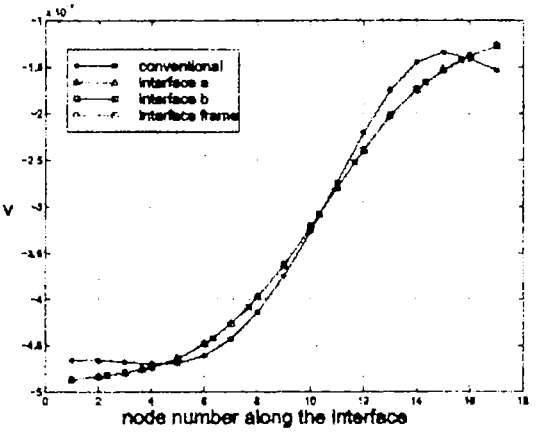

Fig. 15 Vertical displacement v along the interface $(k/E=10^4)$

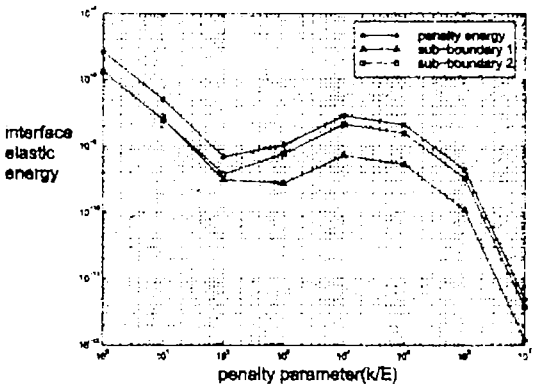

Fig. 16 Elastic energy $\frac{1}{2}k\int_S(\mathbf{v}-\mathbf{u})^2 dS$ caused by penalty constraints

analysis, penalty constraints are imposed too strongly to provide accurate vertical displacements along the interface. They are shown in the Figs. 11 and 15.

The considerable amounts of deviations of displacement fields from the solutions of conventional finite elements are observed. The optimal solution characteristics are investigated by evaluating internal energy of the subdomains for various values of penalty parameter. As shown in the Fig. 16, the optimal solutions of this problem can be obtained at the local minimum of augmented parts of elastic energy $\frac{1}{2}k\int_S(\mathbf{v}^T-\mathbf{u}^T)(\mathbf{v}-\mathbf{u})\,dS$ caused by penalty constraint. However, Further study needs to be followed on how to select proper penalty parameters.

3.4 Plate bending problems

The configuration of the plate under edge bending moments are given in Fig. 17. The nine-node isoparametric Mindlin plate elements are used in the whole domain. The mid-plane is divided into two subdomains. In the subdomain **a**, nine nodes are placed at the interface and in the subdomain **b**, seven nodes are placed at the interface. On the frame interface, 15 nodes are used. Uniform bending moments are applied at the sides of the plate. To eliminate the rigid body modes, transverse deflections w at three corners are set to zero. In Fig. 18, the deformed shape of plate under pure bending is shown.

In the plate bending problem, penalty parameters should be carefully chosen because transverse deflection w and rotational angles θ_x and θ_y have different dimensions. For the given problem, the penalty parameter of vertical displacement is chosen as relatively small (about 10^0) and those of rotational angles are 10^6 times of reference bending rigidity. The number of the nodes on the frame interface is taken as twice as those of boundary nodes of subdomains.

Table 3 shows the comparison between analytical bending patch solutions and the present results. Although the bending patch test cannot be passed rigorously in the present analysis, the

Table 3 Results for pure bending patch test

	w_1	w_2	w_3
Penalty Frame Method	1.0001	0.7001	1.0001
Exact Patch Solution	1.0000	0.7000	1.0000

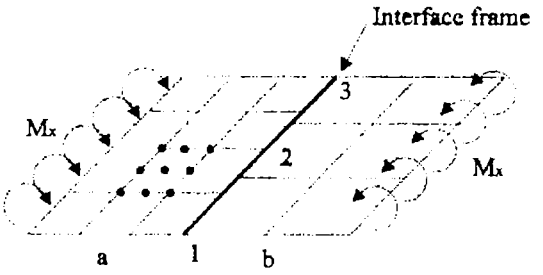

Fig. 17 Plate under pure bending

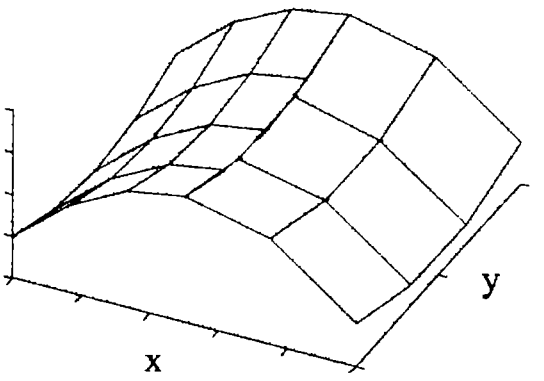

Fig. 18 Deformed shape of plate under pure bending patch test

Table 4 Numerical results for plate flexure

	θ	w_{tip}
Conventional	0°	25.323
Penalty Frame Method	0°	25.310
	10°	25.308
	20°	25.299
	30°	25.276

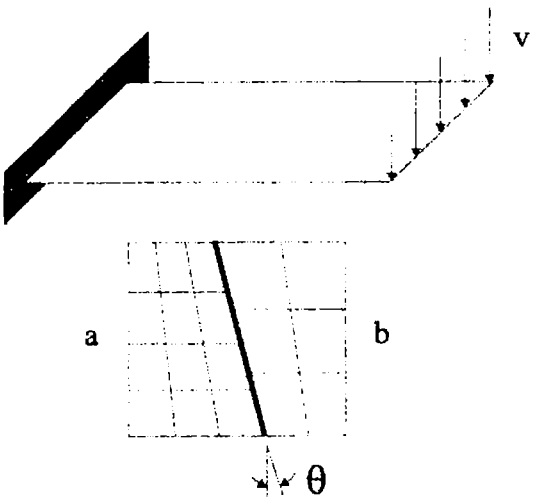

Fig. 19 Clamped plate with a vertical interface under shear force

present penalty frame method works effectively in the coupled analysis.

In the next case, flexure problem is considered. The one end is clamped and the other end is under shear load. To investigate the mesh distortion effect, interface is inclined with angle θ as shown in Fig. 19.

In Table 4, distortion angle θ is varied from 0 to 30 degree by 10 degree increment. The tip deflections are calculated by using nine-node isoparametric elements. As given in Table 4, the present method provides quite accurate end deflections which compares well to the conventional finite element results even in the considerably distorted mesh configurations.

4. Conclusions

The penalty frame method is proposed for the efficient analysis of assembled global structural system, which consists of individual substructures with no mesh compatibilities along the interface. Numerical examples demonstrate the efficiency and accuracy of the proposed method. The present method is simpler in the formulation than the hybrid interface method. Skyline solution algorithm is applicable for the present method since this method provides positive definite banded global symmetric stiffness matrices. The reliable analysis by the present method strongly depends upon the proper selection of penalty parameters. More works need to be followed on how to select proper penalty parameters.

Acknowledgment

This work was supported by the Brain Korea 21 project.

References

Aminpour, M. A. and Krishnamurthy, T., 1997, "A Two-dimensional Interface Element for Multi-domain Analysis of Independently Modeled Three-dimensional Finite Element Meshes," AIAA Paper No. 97-1297, pp. 1853~1861.

Aminpour, M. A., McCleary, S. L., Ransom, J. B. and Housner, J. M., 1992, "A Global/Local Analysis Method for Treating Details in Structural Design," *ASME*, Vol. 157, Adaptive Multilevel and Hierachical Computational Strategies, A. K. Noor(Ed.), pp. 119~137.

Aminpour, M. A., Ransom, J. B. and McCleary, S. L., 1995, "A Coupled Analysis Method for Structures with Independently Modelled Finite Element Subdomains," *Int. J. Nume. Meth. Eng.*, Vol. 38, pp. 3695~3718.

Farhat, C. and Geradin, M., 1992, "Using a Reduced Number of Lagrange Mulipliers for Assembling Parallel Incomplete Field Finete Element Aproximations," *Comput. Meths. Appl. Mech. & Eng.*, pp. 333~354.

Farhat, C. and Roux, F. X., 1991, "A Method of Finite Element Tearing and Interconnecting and its Parallel Solution Algorithm," *Int. J. Nume. Meth. Eng.*, Vol. 32, No. 6, pp. 1205~1228.

Fish, J., 1992, "The S-version of the Finite Element Method," *Computers and Structures*, Vol. 43, No. 3, pp. 173~180.

Krishnamurthy, T. and Raju, I. S., 1992, "An Independent Refinement and Integration Procedure in Multiregion Finite Element Analysis," *AIAA SDM Conference Proceeding*, pp. 109~120.

Ransom, J. B., 1997, "Interface Technology for Geometrically Nonlinear Analysis of Multiple Connected Subdomains," AIAA Paper No. 97-1298, pp. 1862~1872.

Ransom, J. B., McCleary, S. L. and Aminpour, M. A., 1993, "A New Interface Element for Connecting Independently Modeled Substructures," AIAA Paper No. 93-1503.

Robbins, D. H. Jr. and Reddy, J. N., 1992, "Global/Local Analysis of Laminated Composite Plates Using Variable Kinematic Finite Elements," *AIAA SDM Conference Proceeding*, pp. 142~147.

Surana, K. S., 1980, "Transition Finite Elements for Three-dimensional Stress Analysis," *Int. J. Nume. Meth. Eng.*, Vol. 15, pp. 991~1020.

Wang, J. T. and Ransom, J. B., 1997, "Application of Interface Technology in Nonlinear Analysis of a Stitched/RFI Composite Wing Stub Box," AIAA Paper No. 97-1190, pp. 2295~2310.